

## Structure of Trifunctional End-Link Polymer Gels Studied by SANS

E. Mendes,<sup>\*,†</sup> A. Hakiki,<sup>§</sup> J. Herz,<sup>§</sup> F. Boué,<sup>‡</sup> and J. Bastide<sup>§</sup>

Polymer Materials and Engineering, Delft University of Technology,  
 Julianalaan 136, 2628 BL Delft, The Netherlands; Laboratoire Léon Brillouin,  
 CEA-CNRS UMR 12, CEN Saclay, 91191 Gif-sur-Yvette (Cedex), France; and  
 Institut Charles Sadron (CRM-EAHP), 6, rue Boussingault, 67083 Strasbourg (Cedex), France

Received April 2, 2003; Revised Manuscript Received January 30, 2004

**ABSTRACT:** We investigate, using small-angle neutron scattering (SANS), the polymer concentration fluctuations in a particular type of end-linked polystyrene gels, in the swollen state. These gels are obtained from the cross-linking of well-defined end-capped low-polydispersity chains end-linked through a trifunctional cross-linking agent. Polystyrene precursor chains of three different molecular weights, namely 5.5K, 10K, and 15.2K, were used. The scattering at low scattering vectors is expected to come from static concentration fluctuations. Here the intensity displays a dominant scattering characterized either at low  $q$  by a unique correlation length or on a wider  $q$  range by a set of two correlation lengths, one of which has been locked to the correlation length in the semidilute solution of same polymer concentration. We note  $\xi_{\text{het}}$  as a characterization of swelling heterogeneity, the unique low  $q$  correlation length, or the larger one in the double length fit. For both fits, the variation of  $\xi_{\text{het}}$  with the polymer volume fraction  $\phi$  is almost the same for all precursor molecular masses; it scales close to  $\xi_{\text{het}} \sim \phi^{-5/3}$ . Such a variation is surprisingly identical to that observed in “statistical gels” randomly cross-linked from semidilute solutions of very large polymer chains. Results of this paper are thus different from the observations on other end-linking gels, the scattering of which seems to belong to other “classes”, displaying two distinct correlation lengths or a maximum corresponding to soft order between nodule-like junctions.

## 1. Introduction

Since the pioneering permeability experiments in the 1980s by Silberberg,<sup>1,2</sup> polymer gels are known to be heterogeneous in structure. Many different authors carried out detailed investigations during the past decade in such systems, and the major role of heterogeneities in the swelling and deformation of polymer gels was brought into light. In particular, radiation scattering—neutrons, X-rays, light static, and dynamic scattering—was shown by several groups to display an important low  $q$  signal in most of the gels in the presence of solvent, i.e., in the swollen state. Such scattering corresponds to polymer concentration fluctuation at scales comprised between 1 and 100 nm.

On the side of modeling and theory, a lot of attention has also been given to the nature of such large-scale polymer concentration fluctuations, and a large discussion whether they have a thermal or static nature was carried out.<sup>3–9</sup> This paper will not review this debate, but it will start from the present situation. The origin of large-scale polymer concentration in polymer gels is now undeniably established,<sup>10,11</sup> and they can be defined as static polymer concentration fluctuation present in the gel but absent in an equivalent semidilute solution of the same concentration. Using this concept, such mesoscopic structures in polymer gels can be characterized through the excess of scattering intensity with respect to an equivalent semidilute solution. Within this framework, we will discuss the different types of low- $q$  scattering observed on swollen gels, based on our own work as well as on results obtained by other groups.

As a first class of gels, we consider those originating from the cross-linking of semidilute solutions of very

long chains. Their spectra present scattering curves that can be described by one single correlation length,  $\xi$ , as in the case of semidilute solutions. In a previous work,<sup>12,13</sup> the dependence of such a gel correlation length as a function of polymer concentration and cross-link ratio was first experimentally established. This correlation length  $\xi$  has not the same value as that in solution ( $\xi_{\text{sol}}$ ), nor the thermodynamic values  $\xi_{\text{th}}$  expected for those gels from basic theories. Crudely speaking, these two values are masked by the larger correlation length  $\xi$ , in such a way that a single length  $\xi$  is visible. The nature of  $\xi$  for this specific kind of gel (statistical) has been explained by the formation of branched fractal-like hard zones which are interspersed to each other and revealed upon swelling.<sup>3</sup> This desinterspersation mechanism (unscrewing of hard zones) upon swelling is responsible for the excess of scattering of the gel with respect to the semidilute solution. In such a swollen gel, a scattering experiment probes different scales, and the fractal nature of the interspersed hard zones gives rise to a power-law scattering in a very large  $q$  range, until the largest distance between branched structures is reached, saturating the signal at small angles. This swelling process can be mapped on the effect of adding solvent to a set of percolation clusters made by linking short chains, close to the gelation threshold. Close to this threshold, the clusters present a wide distribution of size from the chain size to very large sizes. In a hand-waving picture, one could say that the size of the individual short chains is no longer visible. In statistical gels made from semidilute solutions, the same reasoning can apply, replacing the short chain unit by the blob unit. The model introduces a unique correlation length, and it can indeed account for the observation of one single length in the scattering spectrum. A one  $\xi$  scattering is also observed in the case of aqueous screened polyelectrolyte gels prepared by random radical copolymerization of acrylic acid and *N,N*-methyl-

<sup>†</sup> Delft University of Technology.

<sup>‡</sup> CEA-CNRS.

<sup>§</sup> Institut Charles Sadron.

\* Corresponding author. E-mail: e.mendes@tnw.tudelft.nl.

enebis(acrylamide) in D<sub>2</sub>O, in the presence of a large amount of added salt (responsible for electrostatic screening).<sup>14</sup>

Other classes of polymer gel synthesis have also been investigated. One example is high-functionality junction end-linked gels. In such systems, end-functionalized chains are cross-linked together with a tetrafunctional agent which can either copolymerize with the chains or polymerize with itself. The resulting networks exhibit junctions with functionality much higher than four ("nodules"). At the same time, the scattering spectra belong also to a different class: it presents a pronounced maximum. Such "scattering peak" is similar to that observed in semidilute solutions of high-functionality star polymers.<sup>15,16</sup> In the case of star solutions the higher the functionality, the more pronounced the maximum in the scattering spectrum. As the star functionality decreases, the maximum becomes less pronounced and eventually disappears for very low functionalities. By analogy, we concluded that the gel scattering peak has its origins in the correlation between the high-functionality junctions (or "nodules") which are known to be created in such a gel.

Other end-linked gels of low functionality present, however, a third type of scattering spectrum at small angles: it clearly exhibits two correlation lengths. This feature has been observed by different authors.<sup>11,17–20</sup> In such systems, the smallest correlation length has been associated with the thermal scattering ( $\xi_{th}$ ) and hence, osmotic pressure of the gel, while the larger one,  $\xi_{het}$ , to static heterogeneities. This picture was supported by the good agreement between SANS and light scattering, in particular, the fluctuations of scattered light with the angle and the sample position (speckles). Gels of this kind analyzed in ref 11 were obtained by end-linking of short poly(dimethylsiloxane) chains.

The above scenarios crudely suggest three classes of gels based on their scattering spectrum: (I) the one correlation length gel, as those cross-linked from semidilute solutions, the spectrum of which can be described by one correlation length; (II) the soft order gel, the spectrum of which exhibits a maximum related to a soft colloidal-like order of the junctions; and (III) the two correlation lengths gel where one has been attributed to thermal fluctuations and the other to static polymer concentration fluctuations.

While the nature of the correlation lengths in classes I and II can be described by simple arguments, one is tempted to argue about the nature of the larger correlation length in gels of family III: is it related to a fractal nature, like that of gels cross-linked from semidilute solutions, or is it related to cross-linking defects of chemical or physical nature?

Let us note that the picture of spatial variation of the cross-linking density in statistical gels finds a more general and quantitative theoretical description in the work of Rabin and Panyukov.<sup>8,9</sup> The effect of spatial variations introduced by random cross-linking on the fluctuation of concentration has been calculated within a good order of magnitude. In principle, the model introduces two correlation lengths, analogous to  $\xi_{het}$  and  $\xi_{th}$ . In practice, however, two lengths were not necessary to describe the scattering of the statistical gels studied by us in refs 12 and 15. Moreover, surprisingly, the general shape of the calculated two  $\xi$  curves is more suitable to the scattering of end-linking gels (class III), which are not statistical.

In this background, we looked for the possibility of investigating end-linked gels containing as few defects as possible. The system chosen is synthesized from end-functionalized chains of low polydispersity and very low functionality, namely,  $f = 3$ , and with high expected efficiency in cross-linking. As will be seen below, we have obtained an astonishing result.

## 2. Experimental Section

**Synthesis and Sample Preparation.** Samples were synthesized following the procedure described in detail in refs 21–23. These gels consist of  $\alpha,\omega$ -dihydroethyl-terminated linear polystyrene chains cross-linked by their ends using tris(4-isocyanato)phenylthiophosphate. The reaction was carried out in the presence of diazobicyclooctane (DABCO). End-capped precursor polystyrene chains were synthesized via anionic polymerization and chains of molecular weight of 5.5K, 10K, and 15.2K with polydispersity of the order of 1.01 were used to synthesize gels GET5, GET10, and GET15, respectively. Infrared Fourier transform spectroscopy (IFTR) that permits to follow the disappearance of the C=O bond at the reacting chain end group was used to monitor the reaction. The conversion ratios observed were very large, of the order of 98%. Gel preparation concentration was 27 wt % for all the samples. After synthesis, samples were cut into cylinders and washed in tetrahydrofuran (THF) in a Soxhlet apparatus for 3 days. The amount of extractable nonreacted chains was found to be 1.8, 2.0, and 2.3 wt % for samples GET5, GET10, and GET15, respectively. The extracted amount of nonreacted chains was very consistent with the cross-link conversion rate measured by FTIR, suggesting that almost all nonreacted chains were extracted. The cylindrical gel pieces were then put in excess of toluene in order to exchange the solvent. Samples were put in a new toluene bath every 24 h, and the operation was repeated three times. Cylinders were cut into disks and slowly dried in air. Toluene is less volatile than THF and allows for slow enough drying of the gel. This reduces a lot the risk of damaging the gel disks. After slow drying in air for 1 week, a more thorough removal of the solvent is achieved by bringing the disks to 120 °C in a vacuum for 2 h; they are then slowly cooled back to room temperature. The result was a rather satisfactory disk shape, which is improved to a very homogeneous thickness (monitored by a micrometer screw) using sand paper. The sanded dry disks were then swollen in deuterated solvent directly in the cell used as a container for neutron scattering. The size and thickness of the disks and the weight of added solvent were previously calculated in order to obtain swollen samples that perfectly fit this neutron scattering cell. All solvents were purchased from Aldrich Chemicals and were used without any further purification.

**Neutron Scattering.** Neutron scattering experiments were carried out using spectrometer PACE at Laboratoire Léon Brillouin at Saclay, France. Two spectrometer configurations were used: sample–detector distance of 2 and 4.5 m and neutron incident wavelength of 7 Å. Collimation of the incident neutron beam was achieved in the first case by a 16 mm diaphragm located 2 m before the sample and in the second case using a 12 mm diaphragm at 4.5 m before the sample. Standard procedures for data treatment were carefully applied to raw data, such as normalization by the flat incoherent scattering of water, subtraction of empty quartz cell, and incoherent noise signals.

## 3. Results

Let us first look at data from one gel, GET10, in Figure 1, which displays the scattering spectra, at various swelling degrees  $Q$  in deuterated toluene.

For each swelling degree, comparison is made with a semidilute solution of same polymer volume fraction,  $\phi$  ( $Q \sim 1/\phi$ ). The semidilute solution is used as a reference for homogeneity. Note that although the network of Figure 1 was synthesized from precursor chains of

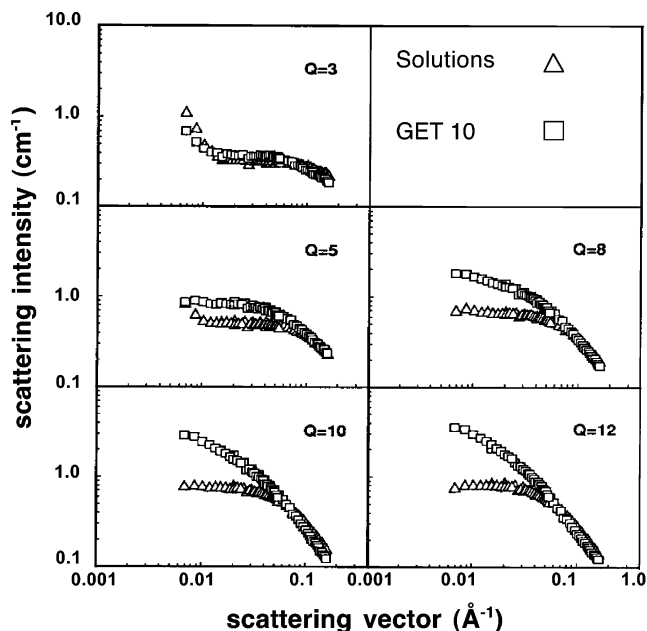


**Figure 1.** Scattering intensity as a function of the scattering vector amplitude for sample GET10 swollen in deuterated toluene at a swelling degrees,  $Q = V/V_0$  (open squares). Semidilute solutions of the same polymer concentrations in toluene are also displayed (triangles). A log–log scale is used in the figure.

molecular weight of 15.2K, data on semidilute solutions of all figures presented in this work are from linear polystyrene chains of molecular weight of 100K. This allows us to have no doubt that solutions are in the semidilute regime, i.e., that concentrations are far above the overlapping concentration ( $\phi \gg \phi^* \sim M^{-0.8} \sim 1\%$  for  $M = 100$  kDa). In this regime, the essential parameter of the system is the correlation length,  $\xi_{\text{sol}}$  (the “blob” size), and depends only on polymer volume fraction,  $\xi_{\text{sol}} \sim \phi^{-3/4}$ .<sup>24</sup> Figure 1 shows that for solutions at large polymer volume fractions (corresponding to  $Q = 3$  and 5) an anomalous scattering appears at  $q$  far smaller than that associated with the correlation length of the solution,  $q^* \sim 1/\xi_{\text{sol}}$ . Such an effect was first reported by Picot and Benoit.<sup>25</sup> Usually, it strongly depends on the preparation history of the solution and increases with molecular weight for a given  $\phi$ .

For a swelling ratio equal to 3, inspection of Figure 1 leads to the conclusion that the scattering of the gel at a polymer volume fraction very close to the one of the preparation state is very similar to that of the semidilute solution of same concentration. The two spectra superimpose for all the scattering vector amplitude range, including the very small angles, where a strong upturn is present for both the gel and the semidilute solution. If this upturn was present only for the gel, it could be related to concentration fluctuations intrinsic to gelation, with a correlation length larger than the one of the solution. This should not be the case here, since the same upturn seems to be present prior to cross-linking.

At lower polymer volume fractions, that is, more diluted solutions or more swollen gels, the anomalous upturn scattering from the solution disappears. At the same time, although the signals from gel and solution superimpose at large  $q$ , the scattering from the gel is larger than the solution one at small  $q$  and levels off at smaller  $q$ . Such excess of scattering of the gel with respect to the semidilute solution of same concentration

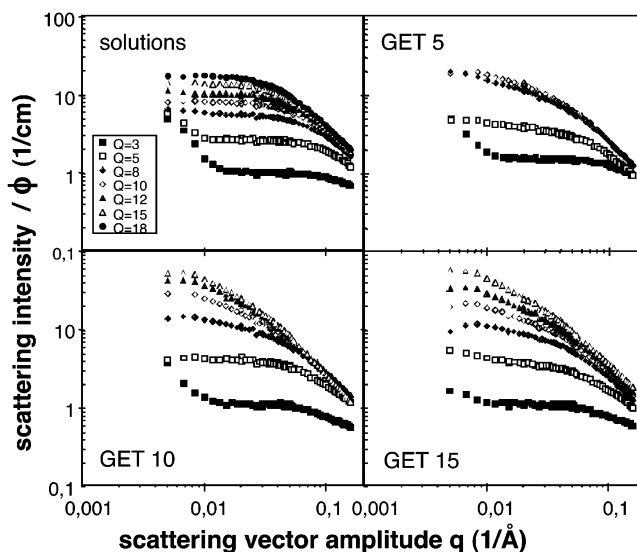


**Figure 2.** Scattering intensity divided by polymer volume fraction,  $I(q)/\phi$ , as a function of scattering vector amplitude for samples GET5, GET10, and GET15. Data for semidilute solutions are also displayed, and the solvent used is deuterated toluene.

is more and more pronounced when the swelling ratio is increased.

Let us now look at data from the three different gels, GET10 as before, plus GET5 and GET15, corresponding to three different molecular weights of precursor chains. This is displayed in Figure 2, where we have divided the scattering intensity by the polymer volume fraction,  $I(q)/\phi$ . Qualitatively, the same behavior is observed in all cases. The curves  $I(q)/\phi$  have the tendency to superimpose at very large  $q$  values, reflecting the local properties of excluded-volume chains, while they level off at smaller  $q$ 's as the swelling ratio increases. It is clearly seen from the figure that the excess scattering with respect to the solutions are very similar at each swelling ratio  $Q$  for the three gels. We have to keep in mind that the swelling range is narrow for GET5 and that the precursor size are relatively close for GET10 and GET15. The similarity is, however, striking.

#### 4. Analysis

We will now analyze the shape of the scattering curves (in  $\log I - \log q$  plot) and fit them to a simple model.

Surprisingly, the shape of the scattering curves for the end-linked gels of this paper is very close to that observed for gels synthesized using random cross-linking of large linear chains in semidilute regime.<sup>12</sup> This is at variance with other gels also synthesized using end-linking methods, which are different from the statistical gels.<sup>12</sup> As said in the Introduction, these other end-linked gels exhibit in their scattering spectra either a colloidal-like scattering maximum (family II)<sup>15,16</sup> or a double-shoulder spectrum with two different characteristic lengths (family III).<sup>11,17–20</sup> In the double-shoulder case, the two lengths have to be different enough to produce a double shoulder. The present end-linked gels scattering display one shoulder, suggesting, therefore, that the correlation length is unique.

**Single  $\xi$  Fitting.** Such a “one shoulder shape” scattering curve prompts us, on a purely experimental basis, to fit the gel scattering data at intermediate and small scattering amplitude values with a Lorentzian-



**Table 1. Correlation Length,  $\xi$  (Å), for the Three End-Linking Gels and Semidilute Solutions at Various Polymer Volume Fractions in Toluene<sup>a</sup>**

correlation length (Å)			single $\xi$ fit			double $\xi$ fit		
$Q$	$\phi$	solutions	GET5	GET10	GET15	GET5	GET10	GET15
3	0.333	3.2	4.9	7.1	6.1	5.1	6.9	8.1
5	0.200	6.0	10.9	11.1	10.4	14.2	12.0	15.3
8	0.125	9.3	29.9	38.4	26.5	35.1	32.5	30.9
10	0.100	11.9		52.1	40.2		53.6	47.9
12	0.083	13.9		55.9	56.8		62.8	65.2
13	0.083	13.9		60.8			66.3	
15	0.067	16.6			68.3			80.6

<sup>a</sup> First set, "single  $\xi$  fit", relates to  $\xi$  extracted from data with a fitting to eq 1. The second set, "double  $\xi$  fit", relates to the larger  $\xi$  extracted from data with a fitting by eq 4.

**Table 2. Scattering Intensity Extrapolated to Zero Wave Vector,  $I(q \rightarrow 0)$  (1/cm), for the Three End-Linking Gels and Semidilute Solutions at Various Polymer Volume Fractions in Toluene<sup>a</sup>**

$I(q \rightarrow 0)$ (1/cm)			single $\xi$ fit			$I(q \rightarrow 0)_{\text{Het}}$			$I(q \rightarrow 0)_{\text{Therm}}$		
$Q$	$\phi$	solutions	GET5	GET10	GET15	GET5	GET10	GET15	GET5	GET10	GET15
3	0.333	0.33	0.51	0.39	0.37	0.45	0.35	0.26	0.06	0.03	0.12
5	0.200	0.52	0.76	0.86	0.74	0.63	0.72	0.55	0.17	0.15	0.24
8	0.125	0.69	1.91	1.93	1.41	1.55	1.30	0.98	0.39	0.46	0.43
10	0.100	0.80		3.16	2.17		2.60	1.62		0.47	0.54
12	0.083	0.86		3.96	3.22		3.40	2.48		0.56	0.67
13	0.083	0.95		4.62			4.15			0.46	
15	0.067	1.00			4.44			3.75			0.74

<sup>a</sup> First data set, "single  $\xi$  fit", relates to that quantity extracted from data with a fitting to eq 1. The second set, columns  $I(q \rightarrow 0)_{\text{Het}}$  and  $I(q \rightarrow 0)_{\text{Therm}}$ , are the two correlation lengths obtained from data fitting by eq 4.

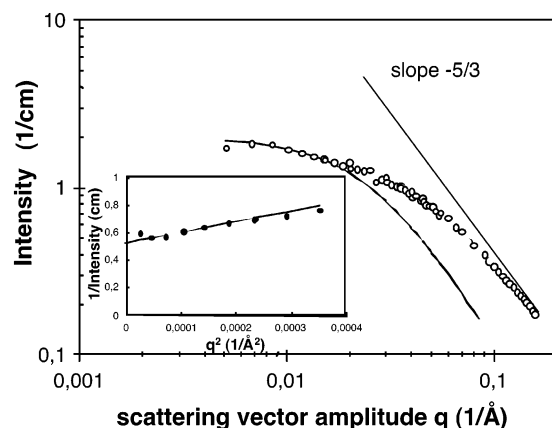


**Figure 3.** Representative example of data set, GET10 at a swelling ratio of  $Q = 8$ , fitted using the "single" correlation length approach. Data and fit are plotted using both representations discussed in the text,  $\log I(q)$  vs  $\log q$  and  $1/I(q)$  vs  $q^2$  (inset).

like curve such as

$$I(q) = [I(0)/(1 + q^2\xi^2)] \quad (1)$$

To extract the correlation length from data, we proceeded as in ref 12. First, from the log-log plots of the intensity as a function of  $q$ , the equivalent of a small-angle Guinier regime (replacing  $R_g$  by  $\xi$ , namely,  $q\xi < 1$ ) is determined: it corresponds in this log-log representation to the plateaulike region observed at low  $q$ . Then, data points in this region are plotted in a Zimm representation,  $1/I(q)$  vs  $q^2$ , and fitted with eq 1, i.e., a straight line. As the gel swells, since the observation window of our measurement is fixed, less and less data points are observed in the so-called Guinier regime. To illustrate this procedure, we choose a representative example of data set, the one of gel GET10 at a swelling ratio of  $Q = 8$ . The scattering data as well as the fitting curves are displayed in Figure 3 where both data representations discussed above are used. Below, we

will discuss an alternative way of fitting to a set of two correlation lengths.

The obtained correlation lengths from fitting to eq 1 are displayed in Table 1, while the intensities extrapolated to zero wave vector are given in Table 2. Let us first note that the correlation lengths obtained for large swelling ratios are far larger than the correlation lengths  $\xi_{R_g}$  associated with the radius of gyration  $R_g$  of the precursor chains in the same solvent ( $\xi_{R_g}^2 = R_g^2/3$  replacing  $\xi^2$  in eq 1, which can then be also used to describe the Guinier range of the scattering from a single Gaussian chain). In dilute solution, using the same procedure as that for the gels, we find  $\xi_{R_g} = 23.4$ , 16.6, and 12.8 Å for precursor chains of  $M_w$  of 15.5K, 10.0K, and 5.2K, respectively. In Figure 4a,b, the correlation length,  $\xi$ , and scattering intensity extrapolated to zero wave vector obtained after fitting,  $I(q \rightarrow 0)$ , are plotted as a function of polymer volume fraction. The correlation lengths for gels with different precursor chain lengths are represented together with the ones from semidilute solutions. The figures suggest that the dependence of  $\xi$  and  $I(q \rightarrow 0)$  with  $\phi$  is almost the same for the three gels studied: the excess scattering does not seem to depend on the molecular weight of the precursor chains. Although the interval of variation of the polymer volume fraction is small, one is tempted to describe  $\xi$ -( $\phi$ ) and  $I(q \rightarrow 0)$ ( $\phi$ ) by power laws. The slopes in Figure 4a,b correspond to  $\xi \sim \phi^{-1.68}$  and  $I(q \rightarrow 0) \sim \phi^{-1.53}$ . We will comment on these exponents below.

**Double  $\xi$  Fitting.** Let us now describe a different fitting of the curves. Let us look at Figure 5, which shows the single  $\xi$  fits for GET10 at the different swelling ratios. Data are well fitted for the low swelling ratios and still well fitted at low  $q$ 's for the larger  $Q$ 's. But when  $Q$  is increased, the fit is correct only at lower and lower  $q$ . One reason can of course be that the validity range of eq 1,  $q < 1/\xi$ , range is more and more narrow. Actually, at  $q > 1/\xi$ , we expect a crossover from eq 1 to a power law variation

$$I(q) \sim q^{-5/3} \quad (2)$$

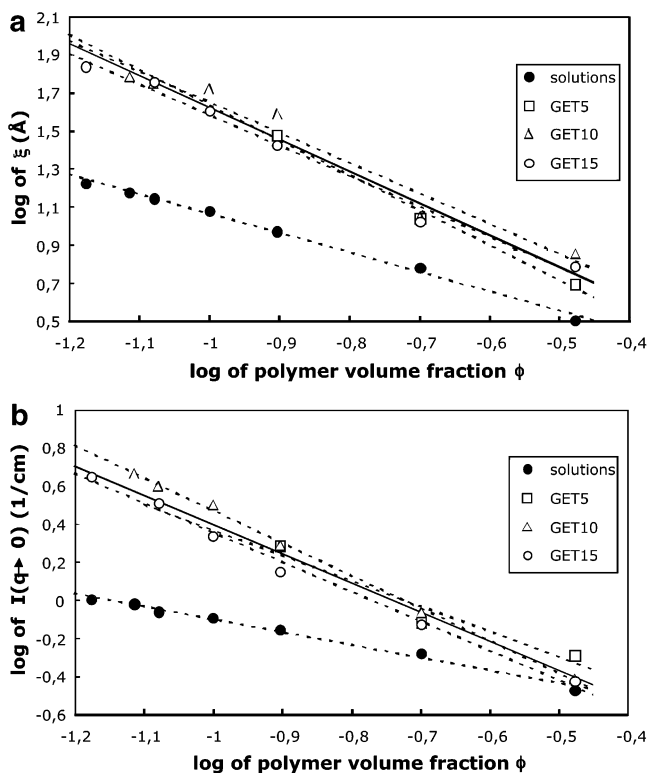


**Figure 4.** (a) Correlation length,  $\xi$  (obtained from the scattering curves as shown above, using the “single” correlation length approach), as a function of polymer volume fraction for samples GET5, GET10, and GET15 and for the equivalent semidilute solutions in deuterated toluene. Dashed lines are fittings to each sample, and the full line is the average of those fittings. (b) Scattering intensity extrapolated to zero wave vector, using the “single” correlation length approach, as a function of polymer volume fraction for samples GET5, GET10, and GET15 and for semidilute solutions. Dashed lines are fittings to each sample, and the full line is the average of those fittings.

different from the  $1/q^2$  variation yielded by eq 1 in the large  $q > 1/\xi$  range. Since  $\xi$  increases with  $Q$ , this  $q$  range will extend by its lower bound. The fits for the largest  $Q$ s, however, are already invalid in a region where the power law is not yet observed; i.e., the scattering is slightly curved in a log–log representation. This suggests that a unique correlation length could not suffice to describe the curve, even if the curves present only one shoulder. We have, therefore, fitted the same data with two correlation lengths, using eq 3:

$$I(q) = [I_1(0)/(1 + q^2\xi_1^2) + I_2(0)/(1 + q^2\xi_2^2)] \quad (3)$$

If we let float all parameters  $I_1$ ,  $\xi_1$  and  $I_2$ ,  $\xi_2$ , the results are slightly scattered. Hence, we decided to impose  $\xi_1 = \xi_{\text{sol}}$ , the value found for the semidilute solution at the same polymer concentration, since these two values  $\xi_1$  and  $\xi_{\text{sol}}$  are, in principle, very close.

$$I(q) = [I_{\text{therm}}(0)/(1 + q^2\xi_{\text{sol}}^2) + I_{\text{het}}(0)/(1 + q^2\xi_{\text{het}}^2)] \quad (4)$$

The obtained values of all the fitted parameters of eq 4,  $\xi_{\text{het}}$ ,  $I_{\text{het}}(0)$ , and  $I_{\text{therm}}(0)$ , are also given in Tables 1 and 2. Inspection of the values of  $I_{\text{therm}}(0)$  in Table 2 clearly indicates that at small swelling ratios the scattering curves exhibit only one scattering length ( $I_{\text{therm}}(0)$  very small), while only for the largest swelling

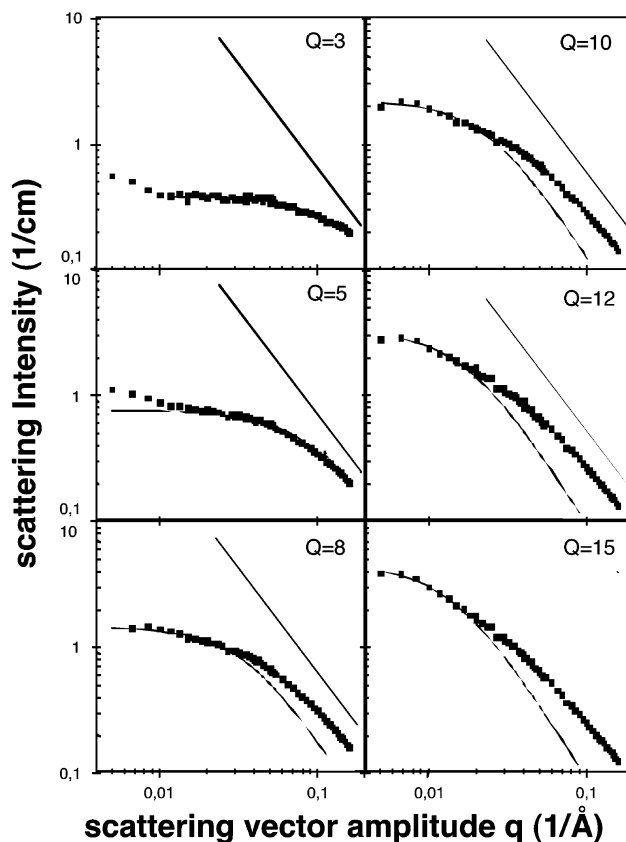


**Figure 5.** Single  $\xi$  scattering fits for GET10 at different swelling ratios. As explained in the text, only very small  $q$  data points are used in the fitting. The slope  $-5/3$  is also represented for each data set.

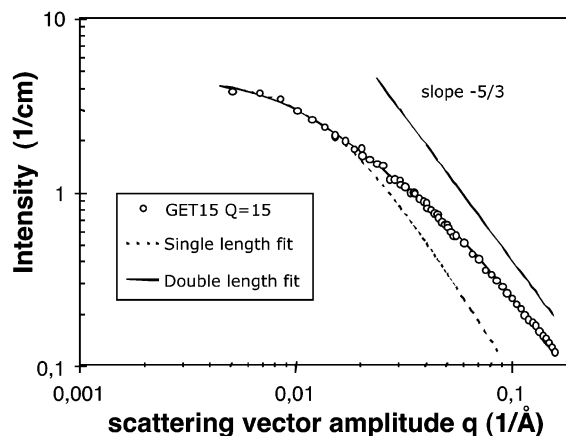


**Figure 6.** Typical representative data curve fitted with two correlation lengths, eq 4. Data corresponds to the scattering of GET15 at a swelling ratio  $Q = 15$ . Dashed line is a fitting curve with a single length while the full curve corresponds to the fitting with two correlation lengths. The slope  $-5/3$  is also displayed.

ratio,  $I_{\text{therm}}(0)$  becomes comparable to the value found in solution.

The obtained values for  $\xi_{\text{het}}$  are not strongly different, but much more systematic. One typical representative curve of fitting from eq 4 is given in Figure 6.

We present  $\xi_{\text{het}}$  and  $I(q \rightarrow 0)$  in log–log plots vs  $\phi$  in Figure 7a,b. The variation can be fitted by straight lines corresponding to  $\xi \sim \phi^{-1.66}$  and  $I(q \rightarrow 0) \sim \phi^{-1.49}$ . These exponents are not very different from the one found for a single  $\xi$  fit. In other words, fitting only the lowest  $q$

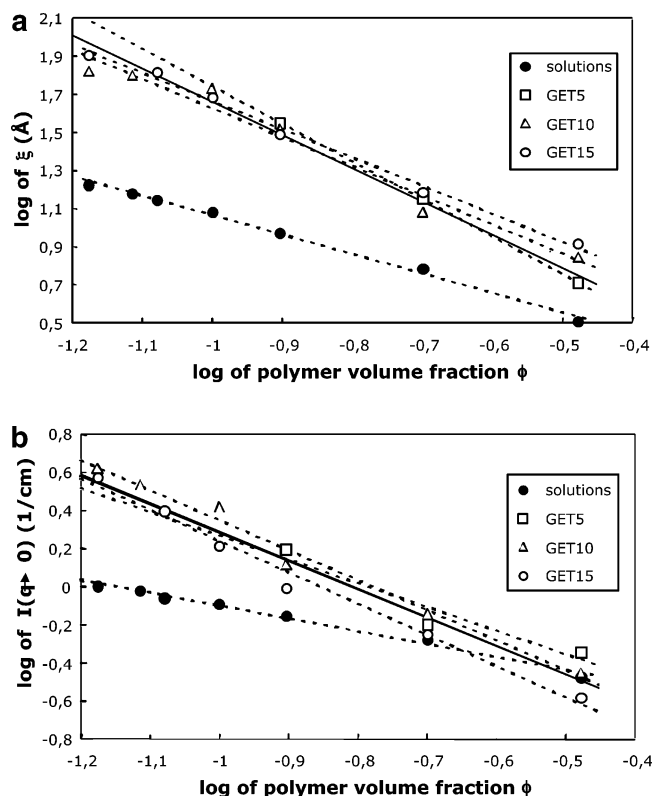


**Figure 7.** (a) Correlation length,  $\xi_{\text{het}}$ , obtained by fitting the scattering curves using the “double” correlation length expression (eq 4), as a function of polymer volume fraction for samples GET5, GET10, and GET15. Also plotted is the correlation length  $\xi_{\text{sol}}$  for the equivalent semidilute solutions in deuterated toluene, at the same polymer concentration.  $\xi_{\text{het}}$  is the largest correlation length found in each fit. Dashed lines are fittings to each sample and full line is the average of those fittings. (b) Scattering intensity extrapolated to zero wave vector of the largest correlation length term of eq 4 (“double” length approach) as a function of polymer volume fraction for samples GET5, GET10, and GET15. Also plotted is the scattering intensity extrapolated to zero wave vector value for the equivalent semidilute solutions in deuterated toluene, at the same polymer concentration. Dashed lines are fittings to each sample, and the full line is the average of those fittings.

range (largest sizes) or fitting a wider  $q$  range gives us similar results for the largest characteristic length.

## 5. Discussion

There are two surprising facts nested in these results, inasmuch as end-linked gels are concerned. The first fact is the “one shoulder” shape of the scattering; such shape is closer to the statistical gels scattering than to other end-linked gels. This can be associated with a unique correlation length. Such interpretation does not assume, however, that other correlation lengths are absent from the gel. It just considers “the most visible” in such a scattering experiment. Such a value is very likely to be different from the one associated with osmotic pressure,  $\xi_{\text{th}}$  which is close to the characteristic length  $\xi_{\text{sol}}$  of a semidilute solution of the same concentration.

Better fits are obtained with two lengths, in particular assuming that the smallest one is equal to  $\xi_{\text{sol}}$ , i.e., the thermal value for fluctuations of concentration in a solution. Introducing a value for osmotic fluctuations in gels (instead of solutions), using the predictions of classical theories, seems difficult in the present case: the fact that the correlation length are not strongly

distinct (one shoulder shape scattering) makes it difficult to estimate a correct average concentration  $\langle \phi \rangle$  to introduce into such classical predicted expressions.

In the background of gel studies recalled in the Introduction, where different “families” were evoked, one can summarize by saying that the scattering of the present end-linked gels is closer to family I of statistical gels than to other end-linked ones (family II and III). The scattering can be described by two correlation lengths, as predicted by the Rabin–Panyukov model which assumes random cross-linking, although the model does not apply, in principle, to the present case, where the large correlation length  $\xi_{\text{het}}$  is very close to the thermal one  $\xi_{\text{th}}$ . The scattering curves in the present study are also not far from predictions of Bastide and Leibler, although they consider only one correlation length, the largest one. In principle, the latter model has been built for very large chains in semidilute regime, i.e., interpenetrated, which are cross-linked randomly.

The second surprise of this work is the apparent exponents for  $\xi(\phi)$  and  $I(q \rightarrow 0)$  vs  $\phi$ . We obtain slightly different exponents for the two ways of fitting:  $-1.68$  and  $-1.66$  for the variation of  $\xi$  with  $\phi$ ;  $-1.53$  and  $-1.49$  for the variation  $I(q \rightarrow 0)$  with  $\phi$ , fitting with one or two correlation lengths, respectively. The obtained exponents are very close to the variations  $\xi \sim \phi^{-5/3}$  and  $I(q \rightarrow 0) \sim \phi^{-5/3}$  first predicted and indeed observed for gels randomly cross-linked from semidilute solutions of very large chains.<sup>3,12</sup> To our knowledge, such a type of dependence of the correlation length with polymer volume fraction is reported here for the first time for gels synthesized through an end-linking method.

The observation of such power laws suggests again a structural similarity with statistical gels and not with other end-linked gels. One is therefore tempted to give the same general interpretation as that for statistical gels: namely, a consequence of the formation of large interspersed hard-to-swell zones in the gel, which are separated in 3 dimensions as the gel is swollen. The variation of the correlation length with polymer volume fraction would correspond to the variation of the average distance between hard zones. The weakness of such interpretation is that, in the one hand, the chains, which are small in the present case, are only slightly entangled, and on the other hand, most of all, randomness cannot arise from the position of the cross-links along the chains, since junctions are bound to be at the end of the chains.

Randomness could come from polydispersity, defects, and chain conformations. Another origin for randomness could be the trapping of entanglements during cross-linking, leading to entanglement concentration fluctuations, and, hence, to zones that are more or less difficult to swell. Let us, however, keep in mind that the average molecular weight between two entanglements in a semidilute solution at  $\phi = 30\%$  could be larger than 100 kDa (since measurements of the storage modulus  $G_N^0$  in the rubbery plateau show that many blobs, ca. 180, are required to create one entanglement).

Besides the above interpretation, the numerical values found for the exponents can be coincidental, simply due to the restricted range of polymer volume fraction of our experiment or to the limited  $q$  range observed (which slightly restricts the accuracy of determination for the largest  $\xi$ ). The narrowness of the concentration window is, however, a consequence of the “good quality”

of the samples, since the precursor chains are short enough ( $<15K$ ) and the polymer concentration in the reaction batch is high enough ( $>25\%$ ). The conversion cross-link ratios of the cross-link reaction are very large, and the sample is very close to a "perfect" network from the chemistry point of view. Gels exhibiting a larger equilibrium swelling degree can be obtained using larger precursor chains and lower polymer concentration during synthesis. Unfortunately, they are very likely to exhibit much more "topological defects" such as dangling and unreacted chains, losing the character of "chemically nearly perfect networks".

## 6. Conclusions

We have reported results on the small-angle neutron scattering of end-linked gels synthesized from end-capped polystyrene chains of low polydispersity with monitored cross-linking. The cross-link agent of functionality equal to 3 was used, and three different precursor chains were considered, namely polystyrene chains of molecular weight of 5.5K, 10K, and 15.2K. Gels were swollen to different swelling degrees in deuterated toluene; for concentrations larger than that of the preparation state, they clearly exhibit an excess of scattering intensity with respect to semidilute solutions of same concentration. Spectra from these end-linked gels present a shape that can be characterized by one "shoulder" in  $\log I - \log q$  plots noticeably different from spectra for other end-linked gels in the literature, which present either clearly two shoulders corresponding to two distinct correlation lengths or a maximum very similar to a "colloidal"-like system.

The shape of the scattering curve can be accounted for with a one characteristic length fit, in the low  $q$  range, or with a two lengths fit over a wider  $q$  range. In the second case, good fits are obtained by imposing the first length to be the same as that obtained for a semidilute solution of same concentration. In the latter case, a strong resemblance with Rabin–Panyukov gel heterogeneities model is encountered. Further comparisons are handicapped by the fact that those models were developed for randomly cross-linked gels exhibiting very distinct correlation lengths.

A similar situation is found for analysis of the variation of the correlation length  $\xi_{\text{het}}$ , as a function of the polymer volume fraction,  $\phi$ : in both one  $\xi$  and two  $\xi$  analysis, it reads as  $\xi_{\text{het}} \sim \phi^{-\alpha}$ , where  $\alpha$  is  $1.67 \pm 0.01$ . This value of  $\alpha$  is very close to that observed in gels randomly cross-linked from semidilute solutions of long chains. The scattering from the latter gels had been interpreted at this time as a consequence from the formation of hard-to-swell zones that are branched and interspersed and which are revealed upon swelling.

In summary, although the swelling ratio (and hence the polymer volume fraction) varies in a narrow range, as it is usually the case for neutral polymer gels, the present results suggest the presence of interspersed hard-to-swell zones in these end-linking gels, similar to those in gels cross-linked from semidilute solutions, despite the difference in architecture between both types of gels.

**Acknowledgment.** The authors thank J. G. Zilliox and F. Isel for their help in the synthesis and characterization of the systems studied here. The referees are also strongly acknowledged for their very constructive comments. We also thank J. Groenewold for fruitful discussions (E.M.)

## References and Notes

- (1) Weiss, N.; Van Vliet, T.; Silberberg, A. *J. Polym. Sci., Polym. Phys. Ed.* **1979**, *17*, 2229.
- (2) Silberberg, A. In *Biological and Synthetic Polymer Networks*; Kramer, O., Ed.; Elsevier Applied Science Series: Amsterdam, 1988.
- (3) Bastide, J.; Leibler, L. *Macromolecules* **1988**, *21*, 2647.
- (4) Rabin, Y.; Bruinsma, R. *Europhys. Lett.* **1992**, *20*, 79.
- (5) Bruinsma, R.; Rabin, Y. *Phys. Rev. E* **1994**, *49*, 554.
- (6) Onuki, A. *J. Phys. Soc. Jpn.* **1989**, *58*, 3065.
- (7) Onuki, A. *J. Phys. II* **1992**, *2*, 45.
- (8) Panyukov, S. V.; Rabin, Y. *Phys. Rep.* **1996**, *269*, 1.
- (9) Panyukov, S. V. *Zh. Eksp. Teor. Fiz.* **1993**, *103*, 1287.
- (10) Mendes, E.; Oeser, R.; Hayes, C.; Boué, F.; Bastide, J. *Macromolecules* **1996**, *29*, 5574.
- (11) Rouf, C.; Bastide, J.; Pujol, J. M.; Schosseler, F.; Munch, J. P. *Phys. Rev. Lett.* **1994**, *73*, 830.
- (12) Mendes, E.; Lindner, P.; Buzier, M.; Boué, F.; Bastide, J. *Phys. Rev. Lett.* **1991**, *66*, 1595.
- (13) Bastide, J.; Mendes, E.; Boué, F.; Buzier, M.; Lindner, P. *Makromol. Chem., Makromol. Symp.* **1990**, *40*, 81.
- (14) Mendes, E.; Schosseler, F.; Izel, F.; Bastide, J.; Boué, F.; Candau, J. *Europhys. Lett.* **1995**, *32*, 273.
- (15) Mendes, E.; Lutz, P.; Bastide, J.; Boué, F. *Macromolecules* **1995**, *28*, 174.
- (16) Marques, C.; Izzo, D.; Charitat, T.; Mendes, E. *Eur. Phys. J.* **1998**, *B3*, 353.
- (17) Horkay, F.; Hecht, A. M.; Mallam, S.; Geissler, E.; Rennie, A. R. *Macromolecules* **1991**, *24*, 2896.
- (18) Horkay, F.; McKenna, G. B.; Deschamps, P.; Geissler, E. *Macromolecules* **2000**, *33*, 5215.
- (19) Shibayama, M.; Takahashi, H.; Nomura, S. *Macromolecules* **1995**, *28*, 6860.
- (20) Takahashi, H.; Shibayama, M.; Fujisawa, H.; Nomura, S. *Macromolecules* **1995**, *28*, 8824.
- (21) Hakiki, A.; Zilliox, J. G.; Beinert, G.; Herz, J. E. *Polymer* **1992**, *33*, 2796.
- (22) Hakiki, A.; Beinert, G.; Herz, J. E. *Polymer* **1992**, *33*, 4575.
- (23) Ramzi, A.; Hakiki, A.; Bastide, J.; Boué, F. *Macromolecules* **1997**, *30*, 2963.
- (24) de Gennes, P. G. In *Scaling Concepts in Polymer Physics*; Cornell University Press: Ithaca, NY, 1979.
- (25) Benoît, H.; Picot, C. *Pure Appl. Chem.* **1966**, *12*, 545.

MA034411M